International Space Planes and Hypersonic Systems and Technologies Conferences
6-9 March 2017, Xiamen, China
21st AIAA International Space Planes and Hypersonics Technologies Conference

Investigation and Control of Unstart Phenomenon in Scramjets

Mohammad Afzal Shadab*[1] and M.F. Baig[2]

Department of Mechanical Engineering, Aligarh Muslim University, Aligarh, India -202001

Engine unstart is generated with the aid of thermal choking due to impulsive heat addition inside the combustor. The generated pressure disturbance traverses upstream inside the isolator duct in the form of normal shock, resulting in a loss of thrust and possible in flameout of the engine. A quasi-one-dimensional adaptation of mass, momentum and energy conservation equations of compressible flow with an appropriate heat release model is employed to investigate the flow physics inside the Scramjet in the case of starting and unstart conditions. Finally, a single-input-single-output (SISO) mechanism based on pressure feedback is proposed to avert this plaguing problem. Pressure enhancement in the upstream propagating normal shock is blown down with the aid of modeled bleeding mechanism. The effectiveness of controlling unstart inside the isolator is further analyzed with varying bleed-length and bleeding efficiency.

Nomenclature

ρ	=	density of the air
t	=	time
e	=	potential energy per unit volume
$\dot{q}$	=	heat release rate
A	=	cross-sectional area
P	=	pressure

* Corresponding author
[1] Undergraduate Student, Department of Mechanical Engineering, Aligarh Muslim University, Aligarh, India - 202001, and AIAA Student Member
[2] Professor, Department of Mechanical Engineering, Aligarh Muslim University, Aligarh, India - 202001

η_c = compression efficiency

$\dot{m}_f$ = mass flow rate of fuel

LHV = lower heating value of the fuel

ϕ = equivalence ratio

f = fuel-air ratio

u = velocity in X-direction

v = velocity in Y-direction

BL = bleed-length

IL = length of the isolator

BE = bleeding efficiency

T = thrust

M = Mach number

h = height of the vehicle from the cowl

γ = specific heat ratio

$\vec{V}$ = velocity vector

$\hat{n}$ = unit vector normal to the cross-sectional area

C_v = specific heat at constant volume

$\dot{m}$ = mass flow rate of air

x = coordinate in X-axis

y = coordinate in Y-axis

k = ratio of mass flow rate of the flow bled to the local mass flow rate of air

R = gas constant for air

Subscripts

o = freestream value

a = air

i = value evaluated at the upstream of the inlet

e = value evaluated at the downstream of the nozzle

st = stoichiometric value

$dynamic$ = dynamic value (for pressure)

hp = heat pulse

iso = evaluated inside the isolator

2 = evaluated at the inlet of isolator

I. Introduction

SUPERSONIC combustion ramjets (Scramjets) have verified their potential for high-speed air-breathing propulsion [1,2] with higher specific impulse than conventional rocket engines [3] and hence are sought to replace the latter in the air transport to enhance the payload delivery of missiles [4] and SSTOs [5]. A tremendous amount of research projects has been performed in order to develop a reliable Scramjet which includes the work of Curran and Stull [6], who proposed the concept of dual mode Scramjet, in order to reduce the operating Mach number range of ramjets. However, due to the intricacies involved and its extreme but narrow operating conditions, it becomes difficult for Scramjets to operate durably [1].

In a ramjet, normal shocks originate inside the isolator [7], which transform to a series of oblique shocks (shock-train) when the Mach number approaches the hypersonic regime. Shock-train inside the isolator aid in adjusting the back pressure at both Ram-Scram operations. If there is a sharp increase in back pressure of the combustor exceeding the stability limits of the inlet and isolator, a transient pressure wave traverses upstream in the isolator. If this flow transience reaches the inlet, it distorts the whole flow field resulting in a significant loss of thrust [8]. This phenomenon is known as Scramjet unstart. Unstart also occurs due to an insufficient mass capture at the inlet due to off-design operations [9].

A significant amount of computational research has been performed on the investigation of unstart in the literature with the aid of three-dimensional solvers [8,10,11], and two-dimensional solvers [10,12,13] along with different techniques [9] in order to reduce the computational cost and time. Quasi-one-dimensional CFD solvers are more computationally cost-efficient and less time-consuming alternatives to understand the flow physics inside the combustor and serve as a viable tool to explore unstart phenomenon. A tremendous amount of research found in literature focuses on unstart investigation and prediction, however, the literature lacks mechanisms to effectively eliminate this plaguing problem.

The present work aims to simulate a complete Scramjet geometry and investigate the prominent unstart problem using quasi-one-dimensional compressible flow solver. Unstart has been generated with the aid of transient heat

pulse inside the combustor. The novelty of the present work lies in the development of a pressure based SISO feedback mechanism to control the unstart phenomena in Scramjets. The system is capable of controlling the engine unstart in a shorter length and hence leads to a reduction in the overall size of the engine. The effects of the design parameters of the proposed scheme on the performance characteristics of the engine are analyzed.

II. Numerical scheme and Scramjet model

A simplified JP-7 fuel powered two-dimensional Scramjet model possessing a design Mach number of 4.00 based on the works of Roberts [14] is assumed in the present work. Since the flow inside the Scramjet external compression inlet fails to qualify as a quasi-one-dimensional phenomenon, a coupled technique is employed in order to yield the flow properties downstream of the inlet. Firstly, design and operating condition are fed to the code for constant dynamic pressure trajectory ($P_{dynamic}$=47,880 N/m^2). An assumption of a three-deflector mixed external-internal compression inlet (four shocks including one back-shock) with an equal amount of deflection is made in the present work. For the designing purpose, the cycle static temperature ratio (T_2/T_0=3.00) is kept constant and the value of the deflector angle is calculated after successive iterations. For off-design Mach numbers, the flow properties are calculated with the aid of $\theta - \beta - M$ relations for the designed angle of deflection. These properties are fed to the quasi-one-dimensional CFD solver. Diagrammatic representation of the Scramjet model is illustrated in Fig.1. The CFD code evaluates flow parameters inside the isolator, combustor, and nozzle where x=0.0 and x=36.096 represent the inlet of isolator and outlet of the nozzle, respectively. The variable area combustor is assumed to have a constant gradient of 3 degrees along with a uniform heat release model followed by a single expansion ramp nozzle (SERN) of 20 degrees' slope.

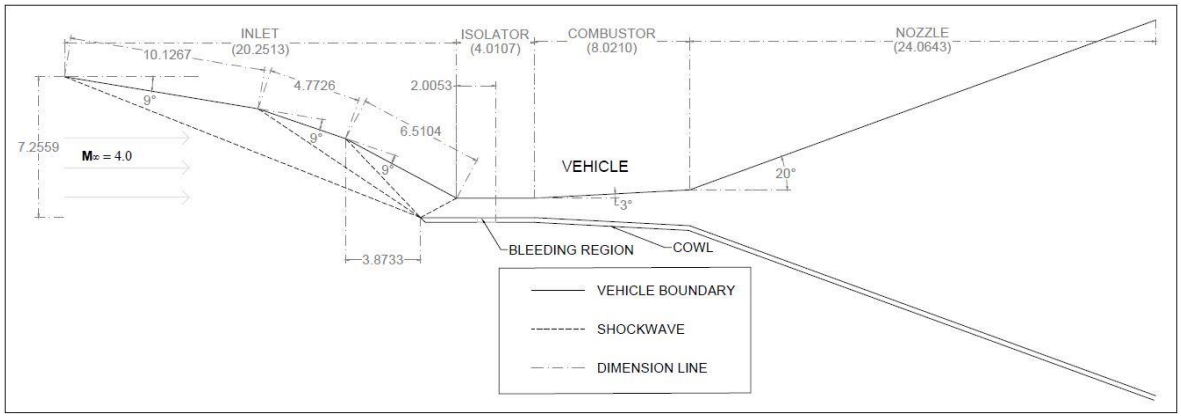

Fig. 1 Geometry of Scramjet considered in the present work

A. Numerical methods

The CFD code employed in the present work is a quasi-one-dimensional finite-difference solver. The conservative form of continuity, momentum and energy equations with a suitable heat addition model is given in equation (1). These equations are valid in the case where unstart controlling mechanism is not actuated.

$$\frac{\partial}{\partial t}\begin{bmatrix}\rho A\\ \rho u A\\ eA\end{bmatrix}+\frac{\partial}{\partial x}\begin{bmatrix}\rho u A\\ (\rho u^2+P)A\\ u(e+P)A\end{bmatrix}=\begin{bmatrix}0\\ P\,(\partial A/\partial x)\\ \dot{q}\end{bmatrix} \tag{1}$$

where heat release ($\dot{q}$) and energy per unit volume (e) are mentioned in equations (2) and (3) respectively. Also, the pressure is related to the temperature and density by the equation of state given in equation (4).

$$\dot{q}=\eta_c\dot{m}_f(LHV)=\eta_c\phi f_{st}\rho u A(LHV) \tag{2}$$

$$e=\frac{P}{\gamma-1}+\frac{1}{2}\rho u^2 \tag{3}$$

$$P=\rho RT \tag{4}$$

Heat release rate is assumed to be directly proportional to the fuel injection rate. The coupled equations in (1) possess a hyperbolic character in time and can yield a spatio-temporal discontinuity in space and time in the presence of a shock wave [3]. Convective terms ρu^2 and eu are spatially discretized with a mix of high & low order upwinding. Time marching is achieved using Euler's time integration, while pressure terms are discretized via central differencing. The flow variables are non-dimensionalized with the freestream variables and length is scaled with the height of isolator as summarized in table 1.

Table 1 Non-dimensionalized variables

Variable	Scaling Variable
ρ	ρ_o
u	u_o
T	T_o
t	h/u_o
x	h
P	$\rho_o {u_o}^2$
$\dot{q}$	$\rho_o {u_o}^2 h$
LHV	$C_v T_o$

The solution is run till t=225.00 on 1081 mesh points with non-dimensionalized steps of $3.422X10^{-2}$ and $7.50X10^{-4}$ in space and time respectively. The combustion efficiency η_C is assumed to be 90% and the simulation achieved a steady state at t=93.00. Non-dimensionalized thrust Υ of the system is evaluated using thrust equation given in equation (5), where $A_e = h_e$ (for unit depth). The only relevant quasi-one-dimensional simulation of Scramjet found in the literature by Goel et al. [3] omitted the pressure thrust due to lack of inlet modeling, which is amended in the present work.

$$\Upsilon = (\dot{m}_e u_e - \dot{m}_i u_i) + (P_e - P_i) A_e \tag{5}$$

B. Unstart generation model

Unstart is generated with the aid of impulsive augmentation in the fuel injection rate (or rate of heat addition). Heat pulse is added for a duration of 7.50 non-dimensional time after the system achieves a steady state at t=93.00. A higher heat addition results in thermal choking inside the combustor, which results in the formation of a normal shock wave at the beginning of the combustor. The normal shock wave travels upstream [3] with the acoustic speed towards the inlet.

C. Controlling of unstart using bleeding mechanism

The generated unstart wave travels upstream to the inlet of the isolator. Due to the formation of a shockwave, a rise of around 8-10 times in pressure is observed in a small distance. Pressure derivative ($\partial P/\partial x$) in space is monitored in the middle of the isolator and when a transient pressure rise is observed, the bleeding mechanism is activated. Bleed-length and bleeding efficiency are the input parameters in the study.

Bleeding is modeled in the transverse direction with the aid of two-dimensional form of continuity equation as given in equation (3). No heat interaction with surroundings is assumed in the present work. By considering the convective loss of mass in transverse direction due to bleeding, the two-dimensional form of continuity equation in conservative form is derived as follows:

$$\frac{\partial(\rho A)}{\partial t} + \frac{\partial(\rho u A)}{\partial x} + \frac{\partial(\rho v A)}{\partial y} = 0 \tag{6}$$

Bleeding is done on the cowl at a height h from the mid-line of the isolator with a velocity v in the transverse direction. A simplified model of convective term in Y-direction is assumed which is as follows:

$$\frac{\partial(\rho A)}{\partial t} = -\frac{\partial(\rho u A)}{\partial x} - \frac{\partial(\rho v A)}{\partial y} \tag{7}$$

$$\frac{\partial(\rho v A)}{\partial y} = \frac{0 - \rho v A_{iso}}{0 - h_{iso}} \tag{8}$$

Let the mass bled in transverse direction be k times the local mass flow rate in streamwise direction at any section. Then by the substitution of equation (8) in equation (7), we get equation (9).

$$\frac{\partial(\rho A)}{\partial t} = -\frac{\partial(\rho u A)}{\partial x} - k\frac{\rho u A_{iso}}{h_{iso}} \tag{9}$$

The pressure-based feedback actuates the bleeding model, thus reducing the local mass and thereby averting the transient normal shockwave to reach the isolator inlet.

D. Boundary conditions

The freestream operating conditions of the Scramjet include a constant dynamic pressure trajectory of $P_{dynamic}$=47,880 N/m^2 rendering a pressure P_i=4275 Pa and T_i=218.33 K for the flight Mach number M=4.0 at a height of 21.65 km from the ground. The stoichiometric fuel-air ratio f_{st} for the JP-7 fuel (LHV=45,903.0 kJ/kg) powered Scramjet is 0.067 and the equivalence ratio ϕ for the operating condition is 0.3. Specific heats at constant pressure and γ are constant and their values are 1005 kJ/kg and 1.362, respectively for air and 1504.846 kJ/kg and 1.238, respectively for the ignited mixture. The employed Riemann boundary conditions are summarized in table 2 for the CFD solver. Outflow and inflow boundary in the domain are identified by the sign of $\vec{V}.\hat{n}$ (outflow if positive and inflow if negative), where $\hat{n}$ is the normal vector to the corresponding domain boundary (x=0.000 and x=36.096).

Table 2 Boundary conditions

Domain Inflow		Domain Outflow	
Subsonic	Supersonic	Subsonic	Supersonic
Specify u, v, T and $\frac{\partial P}{\partial x} = 0$	Specify all variables	$\frac{\partial u}{\partial x} = \frac{\partial v}{\partial x} = \frac{\partial T}{\partial x} = 0$ & specify P	Specify all derivatives

III. Numerical results

Since the phenomenon occurring inside the Scramjet external compression inlet is governed by the presence of two-dimensional oblique shockwaves interaction, it cannot be considered as a quasi-one-dimensional event. So, the inlet simulation is done in the preliminary stage of the code. The inlet has been validated with the results of Roberts

[14] and an accuracy of 0.29% in the angle of deflection is observed for the case where back shock is removed from the code. The rest of Scramjet (CFD model) is validated with the results of Goel et al. [3]. The present work accurately captures flow properties at the downstream of the inlet. The resulting scaled values are indicated where x=0.000, x=4.011, x=12.032 and x=36.096 represent the inlet of isolator, inlet of combustor, outlet of combustor (nozzle inlet) and outlet of the nozzle, respectively.

A. Simulation of quasi-one-dimensional Scramjet

Figure 2 represents the variation of flow parameters inside the Scramjet operating at a Mach number of 4.00 with no unstart present. It is observed from fig. 2 that during combustion, Mach number remains constant inside the isolator but decreases in the combustor due to the heat addition. However, it increases isentropically to 3.7 inside the nozzle. On the other hand, a small rise in pressure inside the combustor is observed, which reduces to low value at the exit of the nozzle. The density reduces in the combustor and then in the nozzle also, while the velocity remains almost constant in the isolator and combustor, but enhances in the nozzle.

B. Investigation of unstart phenomenon

A steady heat pulse of equivalence ratio ϕ_{hp}=3.00 is provided from t=93.00 to t=100.5 after the simulation has reached a steady state. The normal shock formation is not observed until the ϕ_{hp} is increased to 2.40. The shock at lower ϕ_{hp} (i.e. ϕ_{hp}=1.20) remains to sit at the inlet of the combustor but when the ϕ_{hp} is increased to 2.70, the normal shock starts to travel upstream in the combustor. However, the transient normal shock dampens while traversing inside the isolator, thus rendering the isolator useful in decoupling the inlet from the combustion instabilities. It is observed that longer the isolator, higher heat pulses are required to create the unstart, hence longer length of isolators are required to decrease the probability of unstart. Figure 3 represents the traveling of unstart wave from the combustor to the inlet. An abrupt rise in pressure is observed due to the formation of the shock wave, which is also observed from the subsonic Mach numbers in the corresponding regions. The density also increases abruptly, however, the flow velocity decreases drastically. It is observed that a transient disturbance also traverses downstream of the combustor to the nozzle. However, the variations in the flow parameters are not significant when compared with the unstart wave. From fig. 4, it is clear that the unstart occurred faster for the cases of the higher heat pulses. This phenomenon happens due to the development of higher back pressure inside the combustor, which drives the normal shock formation.

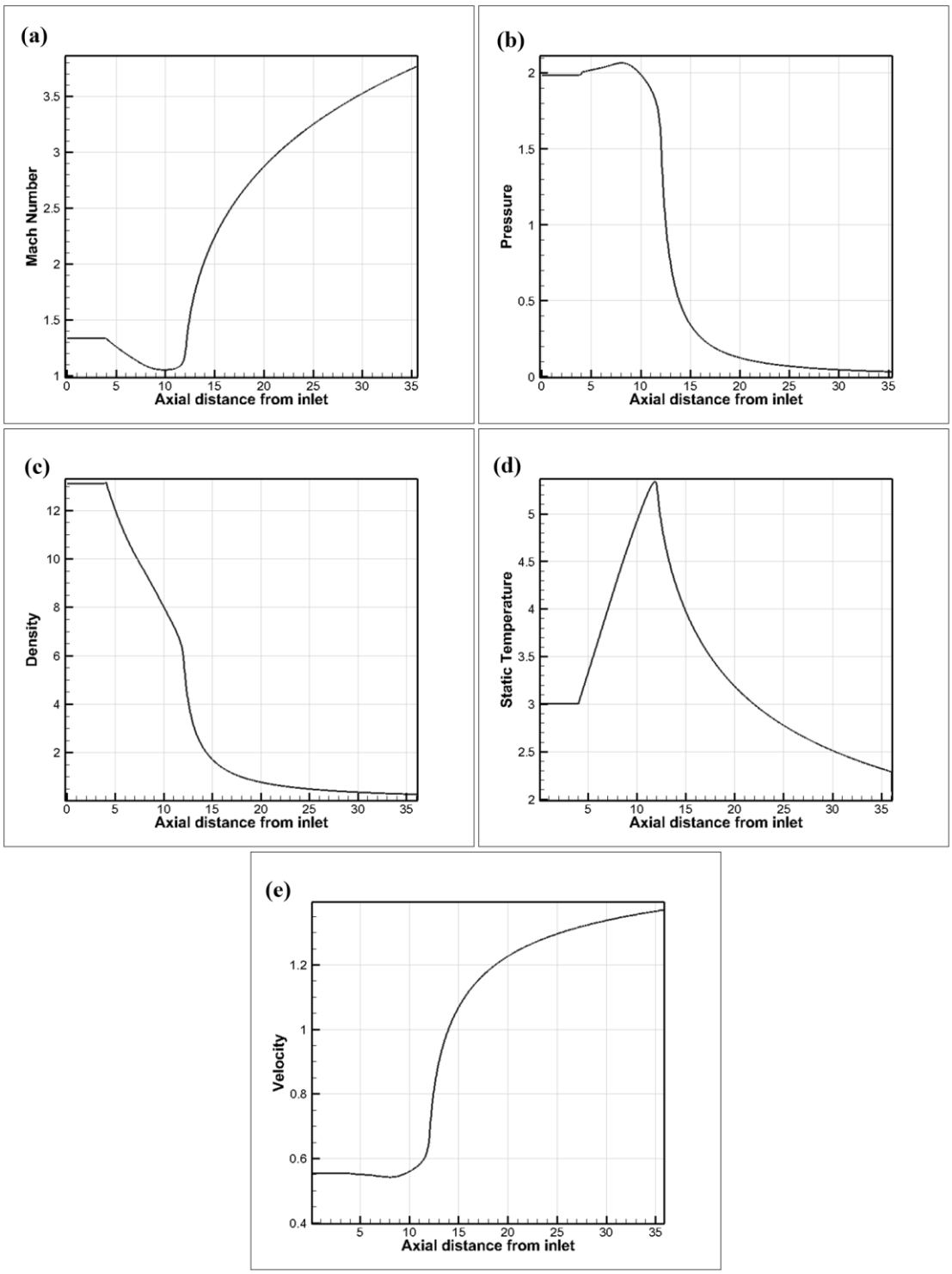

Fig. 2 Distributions of scaled (a) Mach number (b) Pressure (c) Density (d) Static Temperature and (e) Velocity with the scaled axial distance for a quasi-one-dimensional Scramjet operating at M=4.00

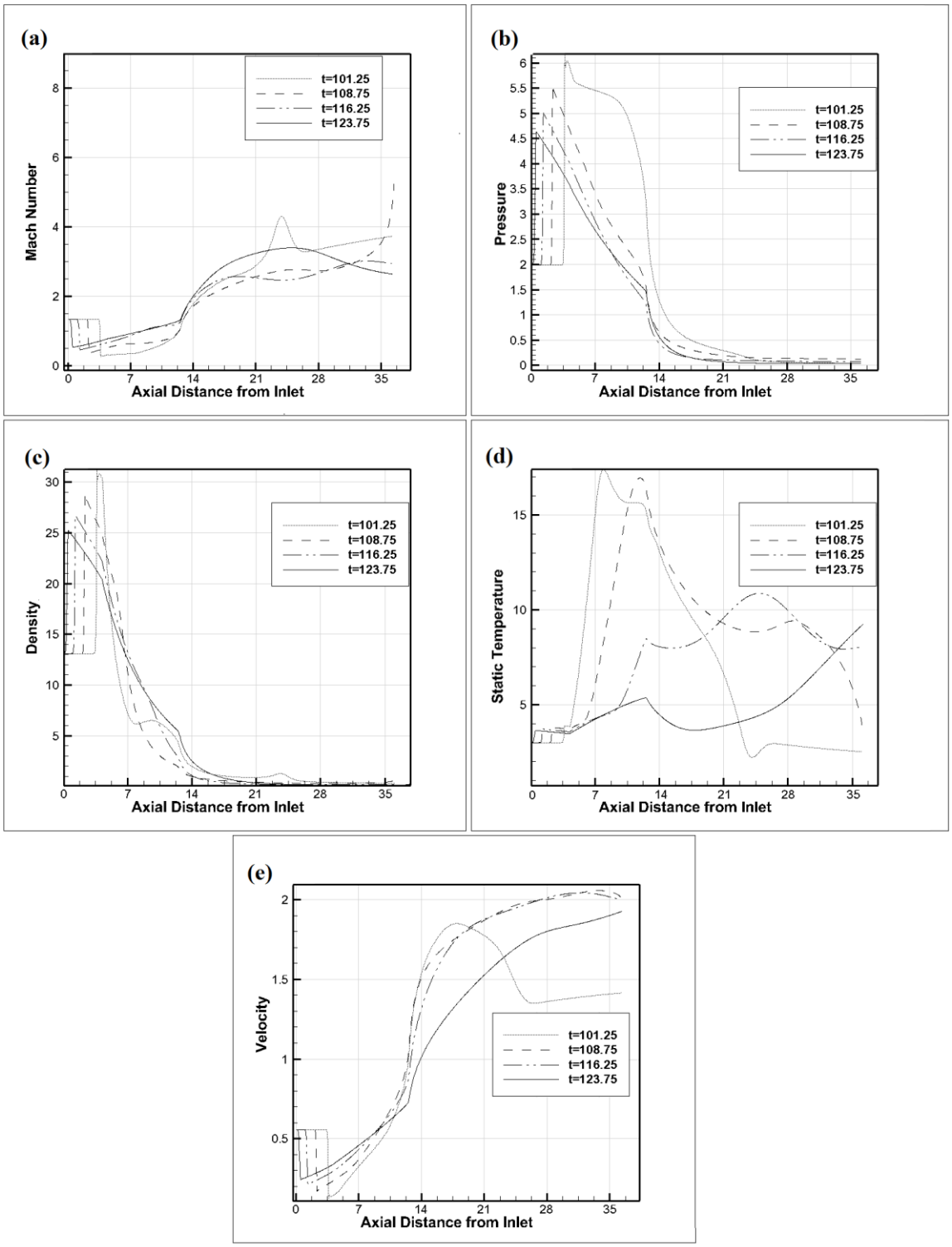

Fig. 3 Distributions of scaled (a) Mach number (b) Pressure (c) Density (d) Static Temperature and (e) Velocity with the scaled axial distance for a quasi-one-dimensional Scramjet operating at M=4.00 in the case of unstart

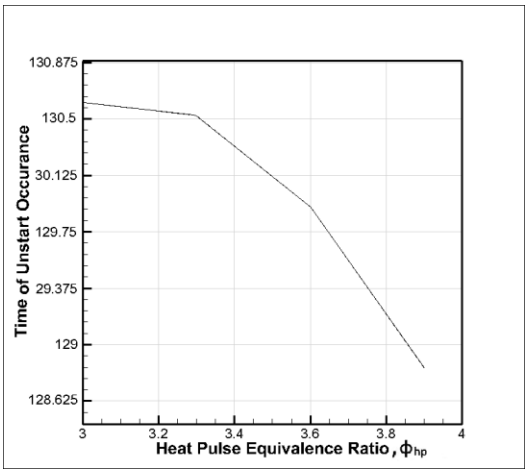

Fig. 4 Variation of unstart occurring time with varying heat pulse equivalence ratios (ϕ_{hp})

C. Controlling the Scramjet unstart using bleeding mechanism

The generated transient unstart wave when it travels upstream activates the bleeding mechanism installed in the middle of the isolator when threshold pressure limit is reached. Fig. 5 shows the variation of flow parameters in x-direction at different instants of time for a heat pulse equivalence ratio of 3.0, bleeding-length of 41.67% of the length of the isolator and a bleeding efficiency of 75.00%. Bleeding efficiency is the percentage ratio of mass bled in transverse with the local mass flow rate in streamwise direction (k%). It is observed that the bleeding resulted in a blowdown of the transient pressure generated inside the isolator. The pressure reduces with time and conversely, the Mach number, and the velocity increase with time. This occurs due to the blowdown of the air from the bleeding region in transverse direction, which aids in mitigating the normal shock.

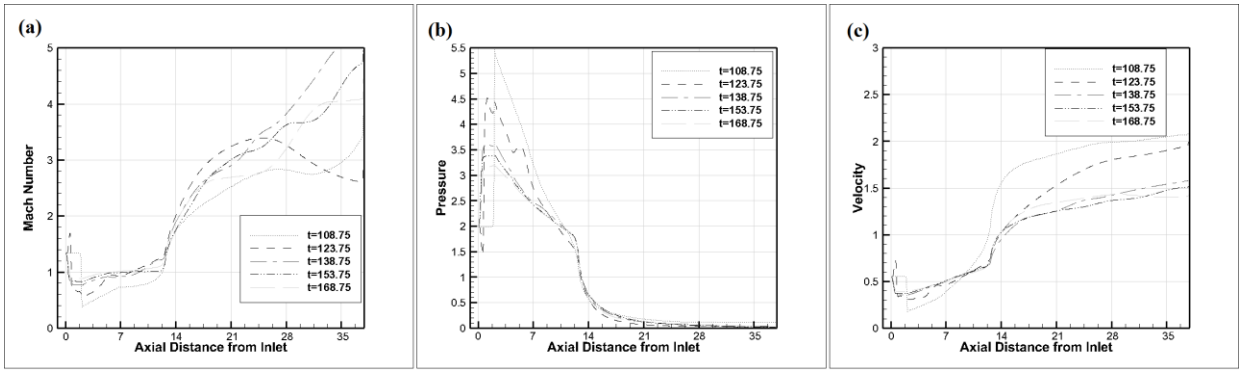

Fig. 5 Distributions of scaled (a) Mach number (b) Pressure (c) Velocity in the case of controlling Unstart at different time steps for ϕ_{hp}=3.0, BL/IL=0.41667, and BE=75%

1. Bleed-length (BL)

The bleed-length plays an important role in designing the mechanism to avert the plaguing problem of engine unstart. A longer bleeding length makes the system more sophisticated, however, a shorter length yields an ineffective blowdown. A steep drop in pressure at the upstream of the isolator is observed from the fig. 6 when the bleed-length to isolator length ratio BL/IL is increased from 0.365 to 0.417. The non-dimensional pressure at the upstream of isolator for BL/IL=0.417 is closer to the isolator pressure (~2.100) for the case of normal running Scramjet condition. Further increasing the BL/IL more than this value yields significantly smaller drop in the peak isolator upstream pressure.

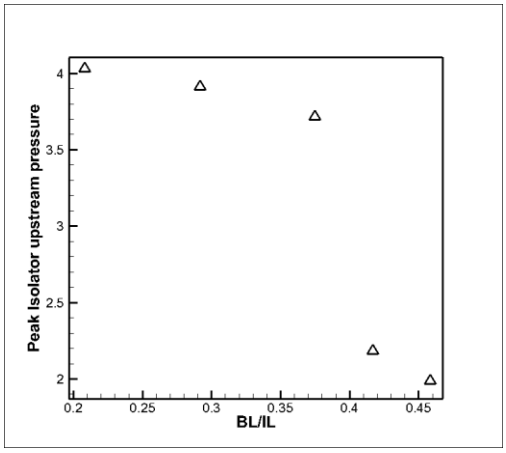

Fig. 6 Peak pressure distribution in the beginning of the isolator with the varying BL/IL for ϕ_{hp}=3.0, and BE=75%

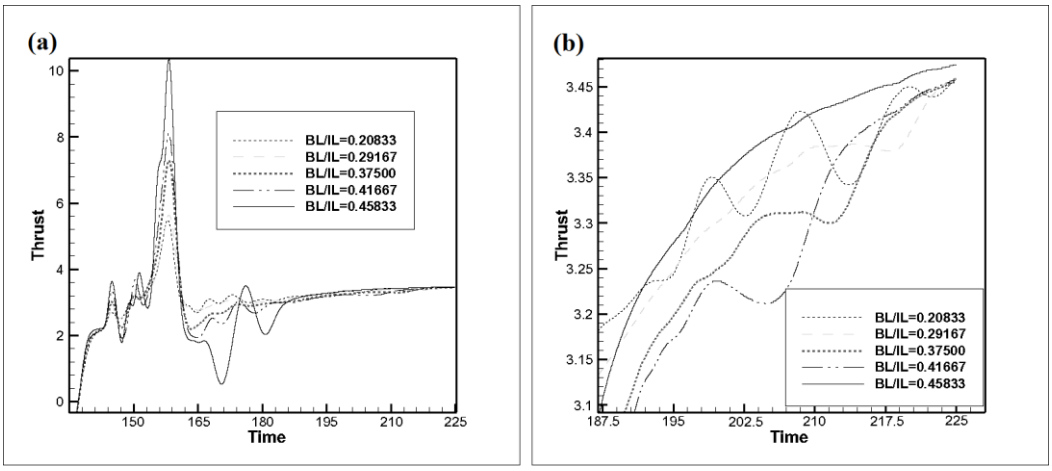

Fig. 7 Transient response of thrust with varying bleed-lengths after occurrence of Unstart for ϕ_{hp}=3.0, and BE=75%

Figure 7 depicts the transient response of thrust with time. It is observed that a positive peak thrust arises, as the flow transients downstream of the bleeding actuators. It is also seen from the thrust response that smaller bleed-length results in a faster thrust adjustment, however, increased bleed-length ensures faster recovery of thrust to its original value.

2. *Bleeding efficiency* (BE)

Bleeding efficiency corresponds to the effectiveness of the amount of bleeding done to avoid the unstart. It is the percentage ratio of mass bled in transverse with the local mass flow rate in streamwise direction (k%). So, the effectiveness of bleeding i.e. bleeding efficiency (BE) needs to be optimized for operating in a specified regime. It is observed from fig. 8 that peak isolator upstream pressure reduces with a rise in the bleeding efficiency. For a bleeding efficiency of 80%, the peak isolator inlet pressure (~2.100) becomes almost equal to the isolator inlet pressure for the case of normal running Scramjet condition. Therefore, the bleeding efficiency for the present case is considered to be 75% for the present case.

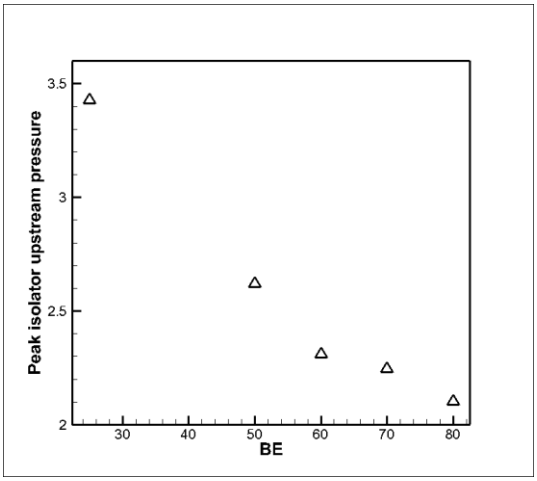

Fig. 8 Peak pressure distribution in the beginning of the isolator with the varying bleeding efficiencies for ϕ_{hp}=3.0, and BL/IL=0.41667

Also, it is illustrated in fig. 9 that thrust adjusts faster for the case of lower bleeding efficiency. A hump is observed due to the transient pressure rise downstream of the bleeding actuators. However, the pressure acquires its original value faster in the case of higher bleeding efficiency and thus is preferred.

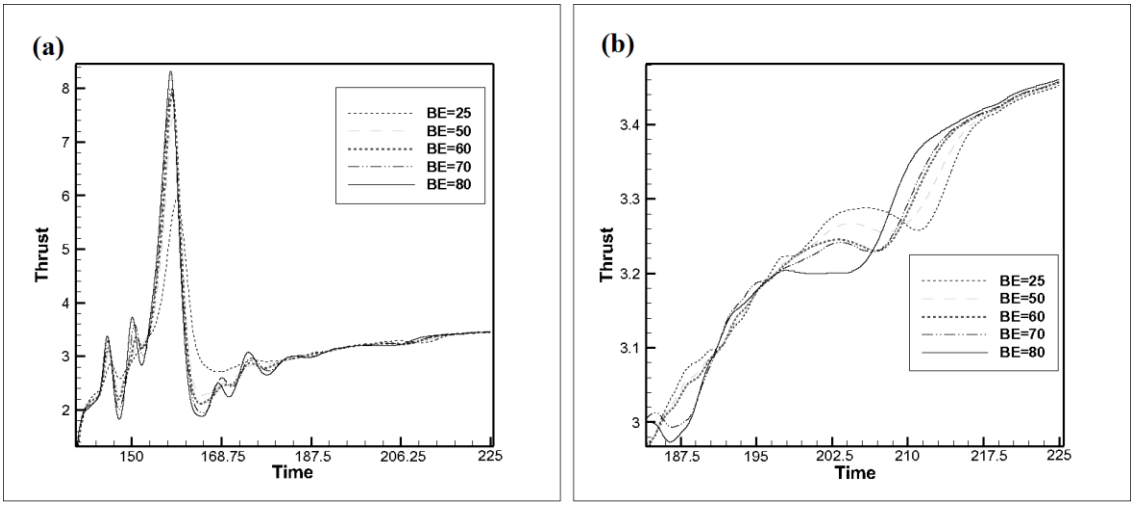

Fig. 9 Transient response of thrust with varying bleeding efficiency after occurrence of Unstart ϕ_{hp}=3.0, and BL/IL=0.41667

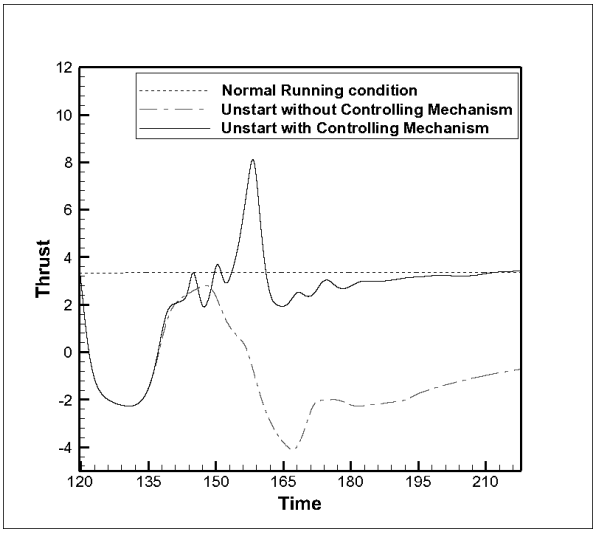

Fig. 10 Comparison of transient thrust response of the Scramjet in the case of normal and unstart (controlled and uncontrolled) conditions for ϕ_{hp}=3.0, BE=75% , and BL/IL=0.41667

Figure 10 depicts a comparison of transient thrust responses for the cases of normal and unstart (controlled and uncontrolled) conditions. A hump is observed in the case of generation of unstart, which is due to the transient pressure and velocity augmentation in the nozzle due to transient heat addition. The thrust then becomes negative since the velocity at the nozzle outlet intensely reduces due to the upstream flow from the combustor towards the inlet. For the case of unstart with actuation of bleeding control, it is seen that the thrust recovers following a transient time period.

IV. Conclusions

A computational study was conducted with the aid of computationally cost-efficient quasi-one-dimensional compressible flow solver on a JP-7 fuel powered Scramjet with a designed Mach number of 4.00. The Scramjet is simulated for the cases of normal running and unstart conditions. Unstart is generated with the aid of heat pulse, which results in a thermal choking inside the combustor leading to upstream propagation of normal shockwave. A novel mechanism for the averting the unstart based on pressure threshold which actuates bleeding mechanism, is proposed and simulated with different bleed design parameters. The following conclusions can be made from the present work:

(1) The length of isolator plays an important role in decoupling the inlet from the combustor. The transient pressure waves dampen in the isolator section. Unstart is generated when the heat pulse is increased above a critical value, which is 2.70 for the present case. Also, a higher heat pulse results in the earlier occurrence of unstart.

(2) Bleeding mechanism paves the way for faster thrust recovery. For the present case, a bleed-length of 41.67% length of the isolator and 75% bleeding efficiency provided almost constant pressure in the beginning of the isolator and the faster pressure recovery. Both bleeding efficiency and bleed-length play a role in the control of the unstart as well as transient thrust variation.

(3) A properly designed bleeding mechanism will reduce the overall length of the isolator and thus, the length of the Scramjet engine. The extension of the present work can be analysis in two and three-dimensions to get a more realistic picture of the underlying phenomenon.

References

[1] Sippel, M. and Klevanski, J., "Preliminary Definition of Supersonic and Hypersonic Airliner Configurations," *14th AIAA/AHI Space Planes and Hypersonic Systems and Technologies Conference*, 2006-7984.

[2] Steelant, J., "LAPCAT: High-Speed Propulsion Technology," *Advances on Propulsion Technology for High-Speed Aircraft*, Vol. 12, 2008, pp.1-12.

[3] Goel, A., Xie, A., Duraisamy, K. and Bernstein, D.S., "Retrospective cost adaptive thrust control of a 1D scramjet with Mach number disturbance," *In 2015 American Control Conference (ACC), IEEE*, 2015, pp.5551-5556.

[4] Kazmar, R. R., "Hypersonic Missle Propulsion System," Tech. rep., *DTIC*, 1998. 1

[5] Chase, R., and M. Tang. "A history of the NASP Program from the formation of the Joint Program Office to the termination of the HySTP Scramjet Performance Demonstration Program." In *International Aerospace Planes and Hypersonics Technologies*, 1995, p.6031.

[6] Wagner, J. L., K. B. Yuceil, A. Valdivia, N. T. Clemens, and D. S. Dolling. "Experimental investigation of unstart in an inlet/isolator model in Mach 5 flow," *AIAA journal*, Vol. 47, No. 6, 2009, pp.1528-1542.

[7] Heiser, W.H., and Pratt, D.T.,"Hypersonic airbreathing propulsion," *AIAA*, 1994.

[8] Jang, I., Pecnik, R., and Moin, P., "A numerical study of the unstart event in an inlet/isolator model, " *Center for Turbulence Research Annual Research Briefs, Stanford University*, 2010, pp.93-103.

[9] Wang, Q., Duraisamy, K., Alonso, J.J. and Iaccarino, G., "Risk assessment of scramjet unstart using adjoint-based sampling methods," *AIAA journal*, Vol. *50*, No. 3, pp.581-592.

[10] Tam, C. J., Lin, K. C., Davis, D. L., & Behdadnia, R., "Numerical investigations on simple variable geometry for improving scramjet isolator performance, "*AIAA paper*, *4509*, 2006.

[11] Su, W.Y., Ji, Y.X. and Chen, Y., "Effects of Dynamic Backpressure on Pseudoshock Oscillations in Scramjet Inlet-Isolator, " *Journal of Propulsion and Power*, Vol. *32*, No. 2, pp.516-528. doi: 10.2514/1.B35898

[12] Jang, I., Moin, P. and Nichols, J.W., "Linear stability analysis of the onset dynamics of scramjet unstart, " *Center for Turbulence Research Annual Research Briefs, Stanford University*, 2015, pp.125-136.

[13] Koo, H., and Raman, V., "Detailed numerical simulations of a supersonic inlet-isolator, " *In Sixth International Symposium on Turbulence and Shear Flow Phenomena, Seoul, South Korea*, 2009, pp.1368-1373.

[14] Roberts, K.N. and Wilson, D.R., "Analysis and design of a hypersonic scramjet engine with a transition Mach number of 4.00, "In *Proceedings of the 47th AIAA Aerospace Sciences, Orlando, FL, USA*, 2009, Vol. 58. doi: 10.2514/6.2009-1255